Genome-wide identification, characterization and expression analysis of *HAK* genes and decoding their role in responding to potassium deficiency and abiotic stress in *Medicago truncatula*

Yanxue Zhao[1], Lei Wang[1], Pengcheng Zhao[2], Zhongjie Liu[3], Siyi Guo[1], Yang Li[1]*, Hao Liu[1]*

[1] State Key Laboratory of Crop Stress Adaptation and Improvement, School of Life Sciences, Henan University, Kaifeng, China
[2] College of Grassland Science, Nanjing Agricultural University, Nanjing, China
[3] Key Laboratory of Genetics and Fruit Development, College of Horticulture, Nanjing Agricultural University, Nanjing, China

Corresponding Author:
Hao Liu
Jinming Road, Kaifeng, Henan, 475004, China
Email address: 10140026@vip.henu.edu.cn
Yang Li
Jinming Road, Kaifeng, Henan, 475004, China
Email address: liyang0378@henu.edu.cn

Abstract

Background. The HAK family is the largest potassium (K^+) transporter family, vital in K^+ uptake, plant growth, and both plant biotic and abiotic stress responses. Although *HAK* family members have been characterized and functionally investigated in many species, these genes are still not studied in detail in *Medicago truncatula*, a good model system for studying legume genetics.

Methods. In this study, we screened the *M. truncatula HAK* family members (*MtHAKs*). Furthermore, we also conducted the identification, phylogenetic analysis, and prediction of conserved motifs of *MtHAKs*. Moreover, we studied the expression levels of *MtHAKs* under K^+ deficiency, drought, and salt stresses using quantitative real-time PCR (qRT-PCR).

33 **Results.** We identified 20 *MtHAK* family members and classified them into three clusters based

34 on phylogenetic relationships. Conserved motif analyses showed that all MtHAK proteins

35 besides MtHAK10 contained the highly conserved K$^+$ transport domain (GVVYGDLGTSPLY).

36 qRT-PCR analysis showed that several *MtHAK* genes in roots were induced by abiotic stress. In

37 particular, *MtHAK15*, *MtHAK17*, and *MtHAK18* were strongly up-regulated in the *M. truncatula*

38 roots under K$^+$ deficiency, drought, and salt stress conditions, thereby implying that these genes

39 are good candidates for high-affinity K$^+$ uptake and therefore have essential roles in drought and

40 salt tolerance.

41 **Discussions.** Our results not only provide the first genetic description and evolutionary

42 relationships of the K$^+$ transporter family in *M. truncatula*, but also provide potential information

43 responding to K$^+$ deficiency and abiotic stresses, thereby laying the foundation for molecular

44 breeding of stress-resistant legume crops in the future.

45

Introduction

47 K$^+$ is an essential macronutrient for various plant physiological functions, like ion homeostasis

48 and the transport of nitrate and sugars (Li et al. 2018). Due to the limited K$^+$ resource, plants

49 have evolved a series of K$^+$ transport systems to mediate its uptake and transport (Amrutha et al.

50 2007; Ashley et al. 2005; Gierth et al. 2005; Very et al. 2014). In plants, K$^+$ transporters are

51 classified into four major families: 1) HAK (high-affinity K$^+$)/KUP (K$^+$ uptake)/KT (K$^+$

52 transporter), 2) Trk/HKT, 3) CHX (cation/hydrogen exchanger), and 4) efflux antiporters KEA

53 (K$^+$ efflux antiporter) (Gupta et al. 2008). Among them, the HAK/KUP/KT (HAK) family

54 constitutes the largest K$^+$ transporter family that is ubiquitously present in plant genomes with

55 varied numbers, e.g., 13 genes present in *Arabidopsis*, 27 in maize, and 27 in rice (Ahn et al.

56 2004; Corratge-Faillie et al. 2010; Gupta et al. 2008; Rubio et al. 2000; Zhang et al. 2012).

57   *HAK* genes have been found to play key roles in plant development and stress-related

58 responses. For instance, *AtKUP4/TRH1* (*Tiny Root Hairs 1*) maintained the polar localization of

59 AtPIN1 along with the auxin homeostasis and maxima in the root apex, thereby promoting root

60 gravitropism response and root hair elongation (Rigas et al. 2001; Rigas et al. 2012; Vicente-

61 Agullo et al. 2004). *VvKUP2* (*Vitis vinifera*) promoted the expansion of berry epidermal cells

62 (Davies et al. 2006). *AtKUP2/SHY3* (*Short Hypocotyl 3*) mediated K$^+$-dependent cell expansion

63 in growing tissues, with the *shy3-1* mutant plants having shorter hypocotyls, smaller leaves, and

64 shorter flowering stems than the wild-type plants (Elumalai et al. 2002b). *Arabidopsis Kup2/6/8*

65 triple mutants displayed larger plant bodies, thus suggesting their roles as negative regulators

66 during the turgor pressure–dependent growth (Osakabe et al. 2013). *Arabidopsis* root meristem

67 activity was maintained by *KUP9* by regulating the K^+ level and auxin homeostasis at a low K^+

68 level (Zhang et al. 2020). *HAK5* promoted the expression of *INTEGRIN-LINKED KINASE1*

69 (*ILK1*) to positively regulate plant innate immunity and abiotic stress response in *Arabidopsis*

70 (Brauer et al. 2016). K^+ deficiency stress induced the expression of rice *OsHAK1*, and when

71 overexpressed in plants they display enhanced salt and drought tolerance (Chen et al. 2015; Chen

72 et al. 2017; Chen et al. 2018). Additionally, constitutive overexpression or mutation analysis of

73 *OsHAK5*, *OsHAK21*, and *OsHAK16* demonstrated their role in K^+ homeostasis and salt tolerance

74 (Feng et al. 2019; Horie et al. 2011; Shen et al. 2015). *HvHAK1* confers salt and drought

75 tolerance in barley by enhancing the leaf mesophyll H^+ homeostasis and improving K^+ nutrition

76 (Feng et al. 2020; Mangano et al. 2008).

77   In plants, the HAK family is the homolog of the bacterial K^+ transporter KUP and fungal K^+

78 transporter HAK (Bañuelos et al. 1995; Schleyer & Bakker 1993; Very et al. 2014). Based on

79 their hydropathy profiles, the plant HAK proteins were predicted to have 10–14 transmembrane

80 (TM) domains, including a conserved K^+ transport domain (GVVYGDLGTSPLY) (Gierth M

81 and Mäser P 2007; Alonso and Rodrı́guez-Navarro 2000). Mutation assay analysis revealed that

82 the role of K^+ transport capacity is determined by both the 8th TM domain and the C-terminus of

83 HAKs (Alonso and Rodrı́guez-Navarro 2000; Gomez-Porras et al. 2012; Mangano et al. 2008).

84 Based on phylogenetic analysis, HAK family genes were generally classified into four clusters

85 (I-IV) (Bañuelos et al. 1995; Gupta et al. 2008). HAK family members exhibit significant

86 diversity in their subcellular localizations, including the plasma membrane, tonoplast,

87 endoplasmic reticulum, and other endomembranes (Osakabe et al. 2013; Rigas et al. 2012).

88 Expression analysis revealed that many members of the HAK family were also expressed in the

89 root hairs and root tip cells, thereby implying the HAK family members are involved in K^+

90 uptake (Ahn et al. 2004; Elumalai et al. 2002b; Qin et al. 2019; Yang et al. 2014). Indeed, several

91 HAK family members have been shown to participate in K^+ uptake and translocation in a few

92 model plants, including *Arabidopsis*, rice, barley, maize, and tomato (Very et al. 2014).

93   *M. truncatula* has been regarded as a model system for studying legume genetics and its

94 relatively small genome size helps understand nodule symbiosis (Young et al. 2011). Despite the

95   functional importance of the HAK genes, surprisingly little is known about their family members

96   in *M. truncatula*. In this study, we performed comprehensive genome-wide analyses of the *M.*

97   *truncatula HAK* family genes including phylogenetic relationships, chromosomal distributions,

98   gene duplications, gene structures, *cis*-acting regulatory elements, and expression patterns in

99   response to both K^+ deficiency and abiotic stress. Finally, these results not only elucidated the

100 structures and expression patterns of 20 *MtHAKs* genes but also laid the foundation for their

101 future functional analysis in *M. truncatula*.

102

Materials & Methods

104 **Identification and sequence analysis of *MtHAKs***

105 *MtHAKs* sequences were obtained from the *Medicago truncatula* genome databases (HAPMAP,

106 https://medicagohapmap2.org). The amino acid (aa) sequences of *Arabidopsis* (TAIR,

107 http://www.arabidopsis.org/) and rice (TIGR, http://rice.plantbiology.msu.edu/) HAKs were used

108 as the reference sequences for searching predicted homolog sequences in *M. truncatula* using the

109 HMMER3.0 software (http://hmmer.org/). Subsequently, the genes were screened using a

110 threshold of < 1e-100 E-value (full sequence and best 1 domain). Candidate protein members

111 were verified using the SMART database (http://smart.embl-heidelberg.de/) and NCBI-

112 Conserved Domain Database (CDD, https://www.ncbi.nlm.nih.gov/Structure/cdd/wrpsb.cgi)

113 (Zhao et al. 2021), with proteins with shorter aa length (< 400 aa) and those containing

114 incomplete K^+ transporter domains being discarded. The longest gene was chosen for further

115 analysis only if it had alternative splicing variants. Subcellular localization of MtHAK proteins

116 was predicted using the WOLF PSORT software (https://www.genscript.com/wolf-psort.html)

117 and the TMHMM Server 2.0 online tool

118 (https://services.healthtech.dtu.dk/service.php?TMHMM-2.0) was used for predicting the protein

119 transmembrane helices.

120 **Construction of MtHAKs phylogenetic tree**

121 HAK protein sequences of *Arabidopsis* and rice were retrieved from the NCBI database

122 (https://www.ncbi.nlm.nih.gov) (Table S1), while multiple sequence alignment was conducted

123 using the ClustalW program (Version 2.1; http://www.clustal.org/). MEGA7.0 was used to

124 construct the phylogenetic tree using the Neighbor-Joining method along with the bootstrap

125 replicates being up to 1000 (Liu et al. 2019; Liu et al. 2020).

126 **Gene structure and conserved motif analysis**

127 Gene structure and conserved motifs were visualized using the TBtools (Toolkit for Biologists

128 integrating various biological data-handling tools) software (Chen et al. 2020). The conserved

129 and identified motifs of protein sequences were predicted via the MEME (Multiple Expectation

130 Maximization for motif Elicitation) program (Version 5.1.1), with the maximum protein motif

131 number being set as 10, and the other parameters set as default (http://meme-

132 suite.org/tools/meme) (Bailey et al. 2009).

133 **Chromosomal location and synteny analysis**

134 The *MtHAK* chromosomal location was illustrated by the circos diagram by annotating genes to

135 their specific chromosomal location in their genome sequences by using the TBtools software.

136 These syntenic analyses were carried out by using the MCScanX with gene duplication

137 parameters (Wang et al. 2012).

138 **Analysis of *cis*-acting regulatory elements in *MtHAKs* promoter regions**

139 Putative *cis*-acting regulatory elements were analyzed using the PlantCARE online software

140 (http://bioinformatics.psb.ugent.be/webtools/plantcare/html/). The 2.0 kb promoter sequences

141 located upstream of the transcription starting site in each *MtHAK* gene were extracted from the

142 *M. truncatula* genome database.

143 **Analysis of microarray expression profile**

144 The microarray data of the expression profiles of *MtHAKs* in the roots, vegetative bud, stem,

145 petiole, leaf, flower, pods, and seeds and their responses to abiotic stress were obtained from the

146 MtGEA (Benedito et al. 2008). When a gene corresponded to multiple probes, the maximum

147 value of the probe was selected for the subsequent analysis. The normalized microarray data was

148 used to create the heatmap through the TBtools software, based on the mean value of each gene

149 expression in all the analyzed organs. The expression patterns of *MtHAKs* in response to salt,

150 drought, and cold stresses were obtained from the NCBI under GEO accession number

151 GSE136739 (Song et al. 2017). The expression abundance of each *MtHAK* gene was represented

152 by fragments per kilobase million (FPKM). The relative stress-induced expression levels were

153 calculated by comparing with the control samples. The clustered heatmap was generated using

154 the TBtools software and based on their relative expression.

155 **Stress treatment and qRT-PCR**

156   For K$^+$ deficiency stress treatment, two-week-old seedlings were grown in 1/2 Hoagland nutrient

157   medium without K$^+$ for 0 (control), 1, 6, 12, 24, and 48 h, respectively. For the salt stress

158   treatment, two-week-old seedlings were grown in 1/2 Hoagland nutrient medium containing 300

159   mM NaCl for 0, 1, 6, 12, 24, and 48 h, respectively. For drought stress treatment, two-week-old

160   seedlings were grown in 1/2 Hoagland nutrient medium containing 18% PEG6000 for 0, 1, 6, 12,

161   24, and 48 h, respectively. The root samples were subsequently cut, then snap frozen in liquid

162   nitrogen, and finally stored at −80°C until further use. The qRT-PCR analysis was performed in

163   triplicates for each of the biological replicates. Their relative expression levels were calculated

164   using the $2^{-\Delta\Delta Ct}$ analysis method (Liu et al. 2019; Zhao et al. 2022). The expression levels of the

165   control samples were normalized to 1, with the *MtActin* gene being used as the internal control.

166   Standard deviations and the significant differences were indicated by error bars and ''*'' *(p <*

167   *0:05),* respectively.

168

169   **Results**

170   **Identification of HAK members in *M. truncatula***

171   To identify *M. truncatula HAK* genes, we conducted a genome-wide search using the

172   HMMER3.0 Software (http://hmmer.org/) based on the *M. truncatula* genome sequences along

173   with the *Arabidopsis* and rice *HAK* genes as subjected queries. Then, we identified 20

174   nucleotide sequences with a typical canonical K$^+$ transporter domain (Pfam accession no.

175   PF02705) using the Pfam and SMART databases, and they were subsequently designated as

176   *MtHAK1* to *MtHAK20* depending on their chromosomal positions (Table 1). Detailed

177   information on the 20 *HAK* genes is listed in Table S1. The number of protein transmembrane

178   segments (TMS) ranged between 10 and 13, with the most common being 12–13 (70%). All the

179   examined HAK proteins were predicted to be mainly localized in the plasma membrane using a

180   PSORT analysis (http://www.psort.org). The protein length of the 20 identified HAK proteins

181   ranged from 619 aa (MtHAK3) to 856 aa (MtHAK2) with an average length of 778 aa. Their

182   relative molecular weights (MW) varied from 69.03 kDa (MtHAK3) to 95.67 kDa (MtHAK2).

183   The isoelectric points (pI) ranged from 5.44 (MtHAK8) to 9.39 (MtHAK19).

184   **HAKs phylogenetic relationship among *M. truncatula*, *Arabidopsis* and rice**

185   To analyze the evolutionary relationships of the MtHAK proteins, we conducted phylogenetic

186   analyses of 60 *HAK* amino acid sequences (20 - *M. truncatula*, 13 - *Arabidopsis*, and 27 − rice)

187   to construct a phylogenetic tree using the Neighbor-Joining method. According to the

188   evolutionary tree, we classified all *HAK* members into four major groups: Groups I–IV.

189   Furthermore, we classified the MtHAK proteins into three clusters (from I to III): Cluster I

190   (MtHAK6, 14, 15, 17, and 18), Cluster II (MtHAK4, 7, 9, 10, 11, 12, 13, 19, and 20), and

191   Cluster III (MtHAK1, 2, 3, 17, 5, and 8) (Figure 1). All members in group IV belong to rice. The

192   most members existed in Cluster II in *M. truncatula*, thus comprising 45% of all MtHAKs. The

193   phylogenetic tree showed that MtHAKs were most closely related to *Arabidopsis* KUPs than

194   those of rice HAKs, thereby indicating that MtHAKs might share evolutionary functional

195   similarities with *Arabidopsis* KUPs. All MtHAKs in cluster I were distributed together with the

196   already-identified AtHAK5, which suggested that they may be crucial for K$^+$ uptake from a low-

197   K$^+$ level soil (Lara et al. 2020). Among cluster II members, MtHAK4 and MtHAK19 shared high

198   sequence identity with AtKUP2 (Elumalai et al. 2002), and AtKUP4 (Rigas et al. 2001; Vicente-

199   Agullo et al. 2004), respectively, thus implying they are likely to be involved in plant

200   development processes. Additionally, among cluster III, MtHAK1 and MtHAK8 clustered

201   together with AtKUP7 (Han et al. 2016), thereby suggesting their role in K$^+$ acquisition and

202   translocation under low K$^+$ concentration.

203   **Gene structure and motif composition of *MtHAK* genes**

204   MtHAK proteins were listed in order based on the phylogenetic analysis (Figure 2A), which was

205   consistent with the results in Figure 1. Closely related members shared similar exon/intron

206   structures, which were related to their biological functions. Gene structures of the *MtHAKs* were

207   abtained based on the arrangement of the untranslated region, exon, and intron sequences

208   generated using the TBTools software. As shown in Figure 2B, the exon number of *MtHAK*

209   genes varied from 8 to 10, and the longest exon existed in the end of a gene except for *MtHAK2*,

210   which is consistent with previous reported data (He et al. 2012; Hyun et al. 2014). Additionally,

211   most *MtHAKs* in the same cluster shared high exon-intron structure similarity (Figure 2B).

212   To study the structural features, we analyzed conserved protein motifs of MtHAKs using

213   the MEME program. We identified the conserved protein motifs varying from 29 to 50 aa in

214   lengths and designated them as motifs 1–10. Conserved protein motif information is shown in

215   Table S2. The highly conserved K$^+$ transport domain (GVVYGDLGTSPLY), included in motif

216   9, existed in all MtHAK proteins besides MtHAK10 (Figure2, Table S2). Motifs 1, 2, 3, 4, 5, 6,

217   7, 8, and 10 were almost evenly distributed along with a feature domain of K$^+$ transporter (Figure

218   2C, Table S2) in all the MtHAK proteins. Therefore, the motifs of conserved K$^+$ transporter and

219   similarities of gene structure in the same cluster together implied the closing function among

220   these HAK members.

Chromosomal distribution and synteny analysis of *MtHAK* genes

222   All identified *MtHAK* genes were mapped onto chromosomes from the *M.truncatula* genome

223   database to identify and locate their chromosomal distribution. Results showed that *MtHAKs*

224   were distributed on seven of the eight chromosomes, with chromosome 8 containing the highest

225   number of six *MtHAK* genes (Figure 3). Five *MtHAK* genes were located on chromosome 5,

226   three on chromosome 2, two on chromosome 4 and 6, one on chromosome 3 and 7, and no gene

227   was allocated on chromosome 1 (Figure 3). These results indicated that *MtHAKs* were scattered

228   randomly onto different chromosome locations.

229   We further performed synteny analysis between *M. truncatula* and *Arabidopsis* to verify the

230   evolutionary relationships and history of the *MtHAK*s. Subsequently, we found seven collinear

231   gene pairs between *M. truncatula* and *Arabidopsis* in the dataset (Figure 3 and Table S3). This

232   indicated that these identified genes might already have existed before protein structure

233   divergence, thereby further implying a strong phylogenetic relationship. Furthermore, only one

234   gene pair (*MtHAK2*/*MtHAK5*) existed as paralogs in *M. truncatula*.

Analysis of *cis*-acting elements in the promoter region of *MtHAK* genes

236   To further investigate the gene function and regulatory mechanism of *MtHAKs*, we analyzed the

237   2 kb regions upstream of the translation start site of the 20 *MtHAK* genes using the PlantCARE

238   database. We identified 73 putative *cis*-elements in the *MtHAK* promoters based on functional

239   annotation, and the major types of *cis*-elements are shown in Figure 4 and Table S4. Post

240   analysis, we identified *cis*-elements corresponding to different plant hormones like auxin (TGA-

241   element and AuxRE-core), gibberellin (GARE-motif and P-box), MeJA (TGACG-motif and

242   CGTCA-motif), ethylene (ERE-box), ABA (ABRE), and salicylic acid (TCA-element), in the

243   promoter regions of all *MtHAKs* genes except *MtHAK20*, thereby suggesting that *MtHAKs*

244   expression may be regulated by different phytohormones. Furthermore, we also found abiotic

245   stress-responsive elements, including STRE, ARE, WRE3, WUN-motif, MBS, LTR, DRE-core,

246   DRE1, and TC-rich repeats, in all the *MtHAKs* promoter regions except *MtHAK20*. Additionally,

247   zein metabolism regulation element (O2-site), endosperm expression element (GCN4-motif and

248   AACA-motif), palisade mesophyll cells element (HD-Zip 1), meristem expression element

249 (CAT-box and CCGTCC-motif), and seed regulation element RY-element were also abundant in

250 the promoter of *MtHAKs* except *MtHAK20*. However, the *MtHAK20* promoter region was

251 abundant in light-responsive elements (Table S4).

252 **Spatial expression profiles of *MtHAK* genes**

253 To gain further insights into the potential biological function of *MtHAK* genes, we used the

254 publicly available microarray data of the *Medicago truncatula* Gene Expression Atlas (MtGEA,

255 https://mtgea.noble.org/v3/) to investigate the temporal and spatial expression pattern of the

256 *MtHAKs*. *MtHAK4* showed relatively high expression in all tissues, while that of *MtHAK18* was

257 low in all tissue (Table S5). Notably, *MtHAK6* and *MtHAK16* were expressed preferentially in

258 the roots, thereby implicating their role in K^+ uptake from the soil (Figure 5, Table S5).

259 Both cluster III genes, *MtHAK2* and *MtHAK3* exhibited similar expression patterns and

260 relatively high expression in leaves. *MtHAK13* was exclusively and highly expressed in floral

261 organs, whereas *MtHAK8* showed the same in immature seeds (Figure 5, Table S5).

262 Interestingly, *MtHAK5* and *MtHAK12* exhibited high and gradually increased expression patterns

263 during the reproductive stages and finally peaked at 24 days after pollination (DAP)

264 Contrastingly, *MtHAK15* was specifically highly expressed in immature seeds (10 DAP) with the

265 expression pattern gradually decreasing along with seed maturation. Therefore, the spatial and

266 temporal expression profiles indicated the functional diversity of *MtHAK* genes in *Medicago*

267 *truncatula* development.

268 **Expression patterns of *MtHAK* genes under K^+ deficiency**

269 Due to the major function of the HAK family being K^+ transport, we investigated the

270 expression profiles of *MtHAK* genes in the roots under K^+ deficient conditions using qRT-PCR.

271 As shown in Figure 6, among the 20 *MtHAK* genes, we obtained eight genes that showed

272 upregulated expression patterns post K^+ deficiency treatment. *MtHAK6*, *MtHAK7*, and *MtHAK17*

273 expression slightly increased and finally peaked at 48 h post treatment. *MtHAK15* and *MtHAK18*

274 showed nearly the same expression pattern at the five different time points. *MtHAK9*, *MtHAK10*,

275 and *MtHAK11* transcripts were strongly upregulated at 6 h, then peaking at 12 h and 24 h, and

276 finally went down at 48 h. Therefore, these results suggested that these *MtHAK* genes were K^+

277 deficiency-responsive. Furthermore, it was noteworthy that *MtHAK6* was highly and specifically

278 expressed in *Medicago trunculata* roots and also significantly upregulated in response to K^+

279 deficiency.

Expression patterns of *MtHAK* genes under salt and drought stresses

Several *HAK* genes have been reported to participate in abiotic stresses (Elumalai et al. 2002; Vicente-Agullo et al. 2004; Chen et al. 2015; Shen et al. 2015). To verify this hypothesis, we evaluated the expression profiles of eight K^+ deficiency responsive genes via qRT-PCR under salt and drought stress treatments. The results revealed that all eight genes were induced by salt and drought stresses to different extents (Figures 7 and 8).

We determined the expression profile of *MtHAK* genes in *Medicago trunculata* roots at different times (0 h, 1 h, 6 h, 12 h, 24 h, and 48 h) under salt treatment (300 mM NaCl in nutrient solution). The results showed that expression of *MtHAK7*, *MtHAK9*, *MtHAK15*, *MtHAK17*, and *MtHAK18* exhibited significant upregulation. Interestingly, *MtHAK7* and *MtHAK18* were quickly and continuously upregulated from 1 h and subsequently increased at 48 h (Figure 7).

Additionally, we analyzed the expression profiles of *MtHAK* genes in *Medicago trunculata* roots under drought treatment simulated by 18% PEG6000 at different times (0 h, 1 h, 6 h, 12 h, 24 h, and 48 h). Under drought treatment, all selected genes besides *MtHAK9* were upregulated, albeit to different levels at different times (Figure 8). In particular, *MtHAK10*, *MtHAK15*, and *MtHAK18* rapidly responded to dehydration at 1 h. Contrastingly, *MtHAK17* was moderately upregulated from 6 h to 48 h. Both *MtHAK6* and *MtHAK7* exhibited highly induced expression at 24 h.

Interestingly, we found that *MtHAK15*, *MtHAK17*, and *MtHAK18* were strongly upregulated by both salt and drought stresses. The expression level of *MtHAK18* increased rapidly at 1 h as compared to the control, under both salt and drought treatments (Figures 7 and 8).

Discussion

HAK family genes play key roles not only in K^+ acquisition and uptake, but also in plant growth, development, and abiotic stress response (Osakabe et al. 2013; Zhao et al. 2016). Although comprehensive genome-wide analysis of the *HAK* gene family has been widely reported in various plants, studies of the *HAK* gene family in the model legume *M. truncatula* were still lacking (Ahn et al. 2004; Gupta et al. 2008; Zhang et al. 2012). The release of the *M. truncatula* genome information makes it possible to systematically characterize and identify the *HAK* genes.

310 In this study, we identified 20 *HAK* genes in *M. truncatula*. We characterized their genetic
311 structures as well as their expression patterns in different tissues and also during stress responses.

312   We classified the 20 identified *HAK* members into three clusters (clusters I to III) based on
313 the evolutionary relationships, which was consistent with the previous classification in
314 *Arabidopsis* (Figure 1) (Rubio et al. 2000). Phylogenetic analysis of HAK proteins revealed that
315 MtHAKs shared higher similarity with AtHAKs as compared to the OsHAKs (Figure 1), thereby
316 suggesting that MtHAKs may share similar functionality with *Arabidopsis* AtHAKs. Gene
317 structure analysis showed that *MtHAK* genes contained 8–10 exons, with the last exon being the
318 longest. However, the exception was *MtHAK2*, which was consistent with the previously
319 reported exon-intron structure of *HAKs* (He et al. 2012; Hyun et al. 2014). Conserved protein
320 motif analysis indicated that all the identified MtHAKs had at least five typical K^+ transporter
321 motifs.

322   The tissue-specific gene expression patterns reflect their function and potential biological
323 roles in plants. Approximately 10 of the 13 *Arabidopsis AtHAK* genes were strongly expressed in
324 the root (Ahn et al. 2004). *MtHAK6* was preferentially highly expressed in the roots, and it
325 belonged to the same clades of *AtHAK5* in the phylogenetic tree, which was also expressed in
326 roots and mediated high-affinity root K^+ uptake (Lara et al. 2020), thereby implicating their role
327 in K^+ acquisition from the soil (Figure 5, Table S5). *MtHAK16* shared high similarity with
328 *AtKUP12*, which showed root hair-specific expression (Ahn et al. 2004). Therefore, these results
329 may help elucidate the biological function of *Arabidopsis* orthologous *MtHAK* genes in K^+
330 acquisition in *M. truncatula*.

331   Some plant *HAK* genes were shown to participate in plant growth and development. For
332 instance, A*tKUP4/TRH1* mutation impaired the root gravitropism response and root hair
333 elongation (Rigas et al. 2001; Rigas et al. 2012; Vicente-Agullo et al. 2004). Knockout of
334 *AtKT2/KUP2* caused shorter hypocotyl length, small rosette leaves, and short flowering stem
335 phenotype (Elumalai et al. 2002). *MtHAK13* was exclusively and highly expressed in the floral
336 organs, while showing low expression levels in other tissues, thereby suggesting its critical role
337 in floral development. *MtHAK5*, *MtHAK8*, *MtHAK12*, and *MtHAK15* were specifically and
338 highly expressed during the reproductive stages, thus implying their roles in facilitating seed
339 maturation and maintaining fertility. The varied tissue expression pattern of the *MtHAK* genes
340 indicated their diverse functions in plants.

341 Under K$^+$ deficiency conditions, plants maintain cytosolic K$^+$ homeostasis by uptaking K$^+$

342 through HAKs, and these K$^+$ transporter genes represent a major transcriptional regulation

343 mechanism during low- K$^+$ stress. AtHAK5 and AtKT1 are two essential transporters mediating

344 high-affinity K$^+$ uptake in the *Arabidopsis* roots, with the roots of their double-mutant unable to

345 sustain plant growth (Lara et al. 2020). ZmHAK5 was characterized as a high-affinity K$^+$

346 transporter in maize (Qin et al. 2019). The expression of OsHAK1 and OsHAK5 were

347 significantly upregulated in roots under low K$^+$ conditions, thereby maintaining the K$^+$ uptake

348 and translocation from the root to the shoot (Chen et al. 2015; Chen et al. 2017; Chen et al. 2018;

349 Yang et al. 2014). We found that K$^+$ deficiency upregulated the root-specific expression of eight

350 *MtHAK*s, especially *MtHAK10* and *MtHAK11* (Figure 6). *MtHAK6* was preferentially and highly

351 expressed in the roots, and it increased under K$^+$ deficiency stress (Figure 6). Therefore, we

352 expect that several *HAK* genes could increase the K$^+$ absorption capacity during K$^+$ deficiency.

353 Previous studies reported that *HAK* genes were crucial for regulating water potential and turgor

354 pressure during osmotic adjustment. These genes also positively regulated plant stress responses

355 by regulating the balance of K$^+$ influx/efflux balance, e.g., *OsHAK1* expression increases in the

356 rice roots post the K$^+$-deficient condition and it positively regulated the salt and drought stress

357 tolerance response (Chen et al. 2015; Chen et al. 2017; Chen et al. 2018). Consistent with the

358 above results, in our study, e.g., *MtHAK7*, *MtHAK9*, *MtHAK15*, *MtHAK17*, and *MtHAK18*

359 exhibited significantly upregulated expression levels in *M. trunculata* roots under salt stress

360 (Figure 7). Interestingly, many *cis*-acting elements related to phytohormones, plant growth and

361 development, and abiotic stress response, were extensively distributed in the promoter regions of

362 the *MtHAKs* (Figure 4). ABREs are drought-stress responsive elements (Sah et al. 2016). *MtHAK*

363 genes contained ABRE elements in their promoters, which further implied that *MtHAKs*

364 participate in drought responses (Figures 4 and 6). Moreover, the qRT-PCR analysis showed that

365 the expressions of most of the selected *MtHAK* genes were noticeably upregulated after drought

366 stress. Notably, *MtHAK6*, which was preferentially highly expressed in the roots, was also

367 significantly upregulated post drought stresses (Figure 8). In particular, the expression of

368 *MtHAK15*, *MtHAK17*, and *MtHAK18* were strongly and specifically upregulated in *M.*

369 *truncatula* roots under K$^+$ deficiency, salt, and drought stress conditions, thus implying that these

370 genes are potential candidates for high-affinity K$^+$ uptake while also being essential in salt and

371 drought tolerance.

372
Conclusions
374   Based on phylogenetic analysis, we identified and characterized 20 MtHAK protein

375 sequences from *M. truncatula* which were grouped into three clusters. Furthermore, we analyzed

376 the chromosome location, conserved protein motif, and gene structure of all the *M. truncatula*

377 *HAK* genes. The *cis*-acting elements regulating plant growth and development, or those

378 responsive to phytohormone and abiotic stress were abundant in the promoter regions of

379 *MtHAKs*. Gene expression analysis assay revealed that *MtHAKs* exhibited diverse tissue-specific

380 expression patterns in various tissues using the publicly available RNA-seq data. Additionally,

381 eight upregulated genes showed varied expression patterns post the K^+ deficiency treatment. The

382 expression pattern analysis under K^+ deficiency, drought, and salt stress suggested that these

383 genes are candidates for high-affinity K^+ uptake that are also crucial in drought and salt

384 tolerance. Therefore, these results provide the first genetic description of the K^+ transporter

385 family in *M. truncatula*, while also laying the foundation for molecular breeding of stress-

386 resistant legume crops in the future.

387
Acknowledgements
389 We would like to thank the reviewers for their comments and suggestion.
390
References

392 **Gierth M and Mäser P. 2007.** Potassium transporters in plants – Involvement in K^+ acquisition,

393   redistribution and homeostasis. *FEBS Letters* **581**:2348-2356.

394 **Ahn SJ, Shin R, and Schachtman DP. 2004.** Expression of KT/KUP genes in *Arabidopsis* and

395   the role of root hairs in K^+ uptake. *Plant Physiology* **134**:1135-1145.

396 **Alonso and Rodríguez-Navarro. 2000.** Potassium transport in fungi and plant. *Biochimica Et*

397   *Biophysica Acta Reviews on Biomembranes*. **1469** (1):1-30.

398 **Amrutha RN, Sekhar PN, Varshney RK, and Kishor PBK. 2007.** Genome-wide analysis and

399   identification of genes related to potassium transporter families in rice (*Oryza sativa L.*).

400   *Plant Science* **172**:708-721.

401 **Ashley MK, Grant M, and Grabov A. 2005.** Plant responses to potassium deficiencies: a role

402   for potassium transport proteins. *Journal of Experimental Botany* **57**:425-436.

403 **Bailey TL, Boden M, Buske FA, Frith M, Grant CE, Clementi L, Ren J, Li WW, and Noble**

404   **WS. 2009.** MEME SUITE: tools for motif discovery and searching. *Nucleic Acids*
405   *Research* **37**:W202-208.

406   **Bañuelos MA, Klein RD, Alexander-Bowman SJ, and Rodríguez-Navarro A. 1995.** A
407   potassium transporter of the yeast Schwanniomyces occidentalis homologous to the Kup
408   system of Escherichia coli has a high concentrative capacity. *Embo Journal* **14**:3021-
409   3027.

410   **Benedito VA, Torres-Jerez I, Murray JD, Andriankaja A, and Udvardi MK. 2008.** A gene
411   expression atlas of the model legume Medicago truncatula. *The Plant Journal* **55**:504-513.
412

413   **Brauer EK, Ahsan N, Dale R, Kato N, Coluccio A, Piñeros MA, Kochian LV, Thelen JJ,**
414   **and Popescu SC. 2016.** The raf-like kinase ILK1 and the high affinity K^+ transporter
415   HAK5 are required for innate immunity and abiotic stress response. *Plant Physiology*
416   **171**(2):1470-1484.

417   **Chen C, Chen H, Zhang Y, Thomas HR, Frank MH, He Y, and Xia R. 2020.** TBtools: an
418   integrative toolkit developed for interactive analyses of big biological data. *Molecular*
419   *Plant* **13**:1194-1202.

420   **Chen G, Hu Q, Luo L, Yang T, Zhang S, Hu Y, Yu L, and Xu G. 2015.** Rice potassium
421   transporter OsHAK1 is essential for maintaining potassium-mediated growth and
422   functions in salt tolerance over low and high potassium concentration ranges. *Plant Cell*
423   *and Environment* **38**:2747-2765.

424   **Chen G, Liu C, Gao Z, Zhang Y, Jiang H, Zhu L, Ren D, Yu L, Xu G, and Qian Q. 2017.**
425   OsHAK1, a high-affinity potassium transporter, positively regulates responses to drought
426   stress in rice. *Frontiers in Plant Science* **8**:1885.

427   **Chen G, Zhang Y, Ruan B, Guo L, Zeng D, Gao Z, Zhu L, Hu J, Ren D, Yu L, Xu G, and**
428   **Qian Q. 2018.** OsHAK1 controls the vegetative growth and panicle fertility of rice by its
429   effect on potassium-mediated sugar metabolism. *Plant Science* **274**:261-270.

430   **Corratge-Faillie C, Jabnoune M, Zimmermann S, Very AA, Fizames C, and Sentenac H.**
431   **2010.** Potassium and sodium transport in non-animal cells: the Trk/Ktr/HKT transporter
432   family. *Cellular and Molecular Life Science* **67**:2511-2532.

433   **Davies C, Shin R, Liu W, Thomas MR, and Schachtman DP**. 2006. Transporters expressed
434   during grape berry (*Vitis vinifera L.*) development are associated with an increase in berry

435  size and berry potassium accumulation. *Journal of Experimental Botany* **57**:3209-3216.

436 **Elumalai RP, Nagpal P, and Reed JW. 2002a.** A mutation in the *Arabidopsis KT2/KUP2*
437  potassium transporter gene affects shoot cell expansion. *Plant Cell* **14**:119-131.

438 **Feng H, Tang Q, Cai J, Xu B, Xu G, and Yu L. 2019.** Rice *OsHAK16* functions in potassium
439  uptake and translocation in shoot, maintaining potassium homeostasis and salt tolerance.
440  *Planta* **250**:549-561.

441 **Feng X, Liu W, Qiu CW, Zeng F, Wang Y, Zhang G, Chen ZH, and Wu F. 2020.** *HvAKT2*
442  and *HvHAK1* confer drought tolerance in *barley* through enhanced leaf mesophyll
443  H($^+$)homoeostasis. *Plant Biotechnology Journal* **18**:1683-1696.

444 **Gierth M, Mäser P, and Schroeder JI. 2005.** The potassium transporter *AtHAK5* functions in
445  K($^+$) deprivation-induced high-affinity K($^+$) uptake and AKT1 K($^+$) channel contribution
446  to K($^+$) uptake kinetics in *Arabidopsis* roots. *Plant Physiology* **137**:1105-1114.

447 **Gomez-Porras JL, Riaño-Pachón D, Benito B, Haro R, Sklodowski K, Rodríguez-Navarro**
448  **A, and Dreyer I. 2012.** Phylogenetic analysis of K$^+$ transporters in bryophytes,
449  lycophytes, and flowering plants indicates a specialization of vascular plants. *Frontiers in*
450  *Plant Science* **3**:167.

451 **Gupta M, Qiu XH, Wang L, Xie WB, Zhang CJ, Xiong LZ, Lian XM, and Zhang QF. 2008.**
452  KT/HAK/KUP potassium transporters gene family and their whole-life cycle expression
453  profile in rice (*Oryza sativa*). *Molecular Genetics and Genomics* **280**:437-452.

454 **Han M, Wu W, Wu WH, and Wang Y. 2016.** Potassium transporter KUP7 Is involved in K($^+$)
455  acquisition and translocation in *Arabidopsis* root under K($^+$)-Limited conditions.
456  *Molecular Plant* **9**:437-446.

457 **He CY, Cui K, Duan AG, Zeng YF, and Zhang JG. 2012.** Genome-wide and molecular
458  evolution analysis of the poplar KT/HAK/KUP potassium transporter gene family.
459  *Ecology and Evolution* **2**:1996-2004.

460 **Horie T, Sugawara M, Okada T, Taira K, Kaothien-Nakayama P, Katsuhara M, Shinmyo**
461  **A, and Nakayama H. 2011.** Rice sodium-insensitive potassium transporter, OsHAK5,
462  confers increased salt tolerance in tobacco BY2 cells. *Journal of Bioscience and*
463  *Bioengineering* **111**:346-356.

464 **Hyun TK, Rim Y, Kim E, and Kim JS. 2014.** Genome-wide and molecular evolution analyses
465  of the KT/HAK/KUP family in tomato (Solanum lycopersicum L.). *Genes & Genomics*

466   **36**:365-374.

467   **Lara A, Rodenas R, Andres Z, Martinez V, Quintero FJ, Nieves-Cordones M, Botella MA,**

468   **and Rubio F. 2020.** *Arabidopsis* K$^+$ transporter HAK5-mediated high-affinity root K$^+$

469   uptake is regulated by protein kinases CIPK1 and CIPK9. *Journal of Experimental*

470   *Botany* **71**:5053-5060.

471   **Li W, Xu G, Alli A, and Yu L. 2018.** Plant HAK/KUP/KT K$^+$ transporters: function and

472   regulation. *Seminars in Cell & Developmental Biology* **74**:133-141.

473   **Liu H, Guo S, Lu M, Zhang Y, Li J, Wang W, Wang P, Zhang J, Hu Z, Li L, Si L, Zhang J,**

474   **Qi Q, Jiang X, Botella JR, Wang H, and Song CP. 2019.** Biosynthesis of DHGA12

475   and its roles in *Arabidopsis* seedling establishment. *Nature Communication*s 10:1768.

476   **Liu Z, Haider MS, Khan N, and Fang J. 2020.** Comprehensive sequence analysis of IQD gene

477   family and their expression profiling in Grapevine (Vitis vinifera). *Genes* **11**(2):235.

478   **Mangano S, Silberstein S, and Santa-María G. 2008.** Point mutations in the barley HvHAK1

479   potassium transporter lead to improved K$^+$-nutrition and enhanced resistance to salt stress.

480   *FEBS Letters* **582**(28):3922-3929.

481   **Osakabe Y, Arinaga N, Umezawa T, Katsura S, Nagamachi K, Tanaka H, Ohiraki H,**

482   **Yamada K, Seo SU, and Abo M. 2013.** Osmotic stress responses and plant growth

483   controlled by potassium transporters in *Arabidopsis*. *Plant Cell* **25**:609-624.

484   **Qin Y, Wu W, and Wang Y. 2019.** ZmHAK5 and ZmHAK1 function in K$^+$ uptake and

485   distribution in maize under low K+ conditions. *Journal of Integrative Plant Biology*

486   **61**(6):691-705.

487   **Rigas S, Debrosses G, Haralampidis K, Vicente-Agullo F, and Hatzopoulos P. 2001.** TRH1

488   encodes a potassium transporter required for tip growth in *Arabidopsis* root hairs. *Plant*

489   *Cell* **13**(1):139-151.

490   **Rigas S, Ditengou FA, Ljung K, Daras G, Tietz O, Palme K, and Hatzopoulos P. 2012.** Root

491   gravitropism and root hair development constitute coupled developmental responses

492   regulated by auxin homeostasis in the *Arabidopsis* root apex. *New Phytologist*

493   **197**(4):1130-1141.

494   **Rubio F, Santa-Maria GE, and Rodriguez-Navarro A. 2000.** Cloning of *Arabidopsis* and

495   barley cDNAs encoding HAK potassium transporters in root and shoot cells. *Physiologia*

496   *Plantarum* **109**:34-43.

497   **Sah SK, Reddy KR, and Li J. 2016.** Abscisic acid and abiotic stress tolerance in crop plants.

498   *Frontiers in Plant Science* **7**:571.

499   **Schleyer M, and Bakker EP. 1993.** Nucleotide sequence and 3'-end deletion studies indicate

500   that the $K(^+)$-uptake protein kup from Escherichia coli is composed of a hydrophobic core

501   linked to a large and partially essential hydrophilic C terminus. *Journal of Bacteriology*

502   **175**:6925-6931.

503   **Shen Y, Shen L, Shen Z, Jing W, Ge H, Zhao J, and Zhang W. 2015.** The potassium

504   transporter OsHAK21 functions in the maintenance of ion homeostasis and tolerance to

505   salt stress in rice. *Plant Cell and Environment* **38**:2766-2779.

506   **Song J, Mo X, Yang H, Yue L, Song J, and Mo B. 2017.** The U-box family genes in Medicago

507   truncatula: Key elements in response to salt, cold, and drought stresses. *PLoS One*

508   **12**:e0182402.

509   **Very AA, Nieves-Cordones M, Daly M, Khan I, Fizames C, and Sentenac H. 2014.**

510   Molecular biology of K^+ transport across the plant cell membrane: what do we learn from

511   comparison between plant species? *Journal of Plant Physiology* **171**:748-769.

512   **Vicente-Agullo F, Rigas S, Desbrosses G, Dolan L, and Grabov A. 2004.** Potassium carrier

513   TRH1 is required for auxin transport in *Arabidopsis* roots. *Plant Journal for Cell &*

514   *Molecular Biology* **40**:523-535.

515   **Wang Y, Tang H, Debarry JD, Tan X, Li J, Wang X, Tae-Ho L, Jin H, Barry M, and Guo**

516   **H. 2012.** MCScanX: a toolkit for detection and evolutionary analysis of gene synteny and

517   collinearity. *Nucleic Acids Research* **40**:e49-e49.

518   **Yang T, Zhang S, Hu Y, Wu F, Hu Q, Chen G, Cai J, Wu T, Moran N, Yu L, and Xu G.**

519   **2014.** The role of a potassium transporter OsHAK5 in potassium acquisition and

520   transport from roots to shoots in rice at low potassium supply levels. *Plant Physiology*

521   **166**:945-959.

522   **Young ND, Debelle F, Oldroyd GED, Geurts R, Cannon SB, Udvardi MK, Benedito VA,**

523   **Mayer KFX, Gouzy J, Schoof H, Van de Peer Y, Proost S, Cook DR, Meyers BC,**

524   **Spannagl M, Cheung F, De Mita S, Krishnakumar V, Gundlach H, Zhou SG,**

525   **Mudge J, Bharti AK, Murray JD, Naoumkina MA, Rosen B, Silverstein KAT, Tang**

526   **HB, Rombauts S, Zhao PX, Zhou P, Barbe V, Bardou P, Bechner M, Bellec A,**

527   **Berger A, Berges H, Bidwell S, Bisseling T, Choisne N, Couloux A, Denny R,**

528   **Deshpande S, Dai XB, Doyle JJ, Dudez AM, Farmer AD, Fouteau S, Franken C,**
529   **Gibelin C, Gish J, Goldstein S, Gonzalez AJ, Green PJ, Hallab A, Hartog M, Hua A,**
530   **Humphray SJ, Jeong DH, Jing Y, Jocker A, Kenton SM, Kim DJ, Klee K, Lai HS,**
531   **Lang CT, Lin SP, Macmil SL, Magdelenat G, Matthews L, McCorrison J,**
532   **Monaghan EL, Mun JH, Najar FZ, Nicholson C, Noirot C, O'Bleness M, Paule CR,**
533   **Poulain J, Prion F, Qin BF, Qu CM, Retzel EF, Riddle C, Sallet E, Samain S,**
534   **Samson N, Sanders I, Saurat O, Scarpelli C, Schiex T, Segurens B, Severin AJ,**
535   **Sherrier DJ, Shi RH, Sims S, Singer SR, Sinharoy S, Sterck L, Viollet A, Wang BB,**
536   **Wang KQ, Wang MY, Wang XH, Warfsmann J, Weissenbach J, White DD, White**
537   **JD, Wiley GB, Wincker P, Xing YB, Yang LM, Yao ZY, Ying F, Zhai JX, Zhou LP,**
538   **Zuber A, Denarie J, Dixon RA, May GD, Schwartz DC, Rogers J, Quetier F, Town**
539   **CD, and Roe BA. 2011.** The Medicago genome provides insight into the evolution of
540   rhizobial symbioses. *Nature* **480**:520-524.

541   **Zhang ML, Huang PP, Ji Y, Wang S, Wang SS, Li Z, Guo Y, Ding Z, Wu WH, and Wang**
542   **Y. 2020.** KUP9 maintains root meristem activity by regulating K^+ and auxin homeostasis
543   in response to low K. *EMBO Reports* **21**(6):e50164.

544   **Zhang Z, Zhang J, Chen Y, Li R, Wang H, and Wei J. 2012.** Genome-wide analysis and
545   identification of *HAK* potassium transporter gene family in maize (*Zea mays L.*).
546   *Molecular Biology Reports* **39**:8465-8473.

547   **Zhao P, Liu Y, Kong W, Ji J, Cai T, and Guo Z. 2021.** Genome-wide identification and
548   characterization of calcium-dependent protein kinase (*CDPK*) and *CDPK-related kinase*
549   (*CRK*) gene families in *medicago truncatula*. *International Journal of Molecular Science*
550   **22**(3):1044.

551   **Zhao S, Zhang M-L, Ma T-L, and Wang Y. 2016.** Phosphorylation of ARF2 relieves Its
552   repression of transcription of the K^+ transporter gene *HAK5* in response to low potassium
553   stress. *Plant Cell* **28**:3005-3019.

554   **Zhao Y, Wang L, Sun X, Bao Y, Liu H, and Zhao Y. 2022.** Inhibition of ribosome biogenesis
555   by actinomycin D affects Arabidopsis root development. *Biochem Biophys Res Commun*
556   588:61-67.

Characteristics of *MtHAK* genes in *M. truncatula*

Gene name	Gene ID	No. of aa	MW (kDa)	pI	TMS	Subcellular localization
MtHAK1	Medtr2g008820.1	849	94.74	5.66	11	PM
MtHAK2	Medtr2g438150.1	856	95.67	8.26	13	PM
MtHAK3	Medtr2g438160.1	619	69.03	9.28	13	PM
MtHAK4	Medtr3g094090.1	794	89.3	7.24	13	PM
MtHAK5	Medtr4g094660.1	787	88	8.08	13	PM
MtHAK6	Medtr4g099260.1	815	90.92	8.74	11	PM
MtHAK7	Medtr5g034500.1	782	87.25	8.24	13	PM
MtHAK8	Medtr5g070670.1	849	95.05	5.44	12	PM
MtHAK9	Medtr5g071630.1	725	81.46	6.63	12	PM
MtHAK10	Medtr5g071827.1	666	74.26	7.22	10	PM
MtHAK11	Medtr5g071860.1	754	84.24	7.02	11	PM
MtHAK12	Medtr6g007697.1	776	87.1	7.71	13	PM
MtHAK13	Medtr6g033165.1	819	91.56	8.71	12	PM
MtHAK14	Medtr7g108480.1	773	87.24	7.77	12	PM
MtHAK15	Medtr8g022130.1	766	85.45	7.77	12	PM
MtHAK16	Medtr8g063840.1	840	93.11	6.51	12	PM
MtHAK17	Medtr8g063900.1	745	83.49	8.45	11	PM
MtHAK18	Medtr8g088200.1	782	87.17	9.03	10	PM
MtHAK19	Medtr8g099090.1	792	88.52	9.39	12	PM
MtHAK20	Medtr8g107510.1	782	86.83	8.32	12	PM

1   aa, amino acid; MW, molecular weight; pI, isoelectric points; TMS, transmembrane segments;

2   PM, plasma membrane.

Figure 1

Phylogenetic analysis of HAK proteins in *M. truncatula* (red circle), *A. thaliana* (green triangle), and *O. sativa* (blue square).

The tree was constructed using MEGA7.0 software by the Neighbor-Joining method. The numbers next to the branch represent the 1000 bootstrap replicates expressed in percentage.
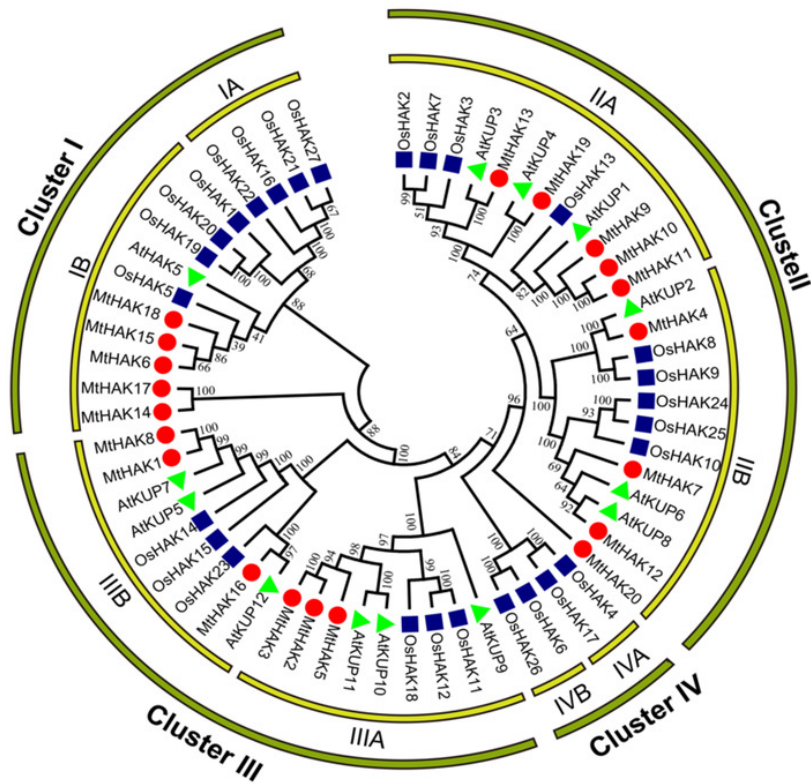
Figure 2

Phylogenetic tree, gene structure, and conserved motifs of the HAKs in *M. truncatula*.

(A) Phylogenetic tree of the MtHAK proteins. (B) Exon-intron structure distribution. (C) Conserved protein motifs.
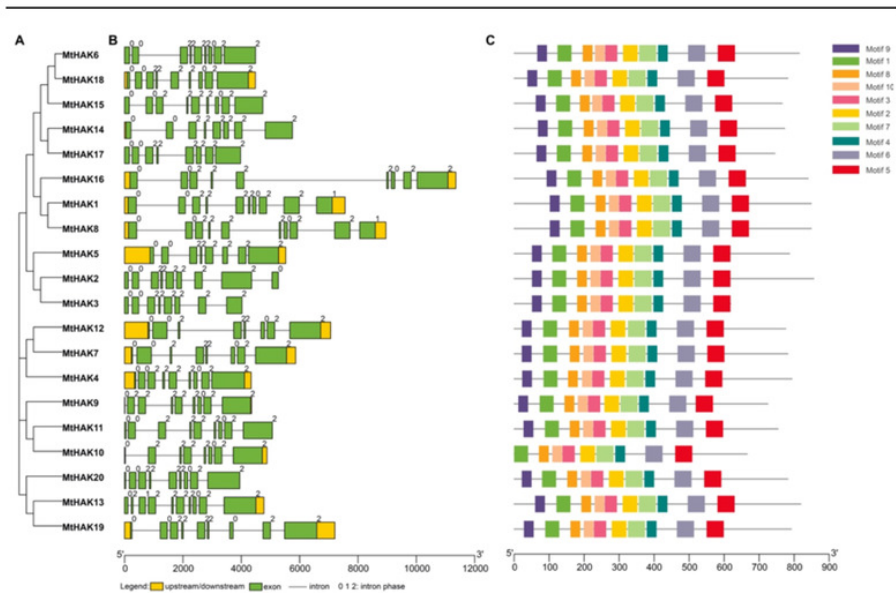
Figure 3

The synteny analysis of MtHAKs displayed between the *M. truncatula* and *Arabidopsis* genomes.

The *M. truncatula* and *Arabidopsis* chromosomes are represented by yellow and green boxes, respectively. Blue lines indicate the collinear relationship of *MtHAKs* between *M. truncatula* and *Arabidopsis*, while green lines indicate the *MtHAK* gene pairs.
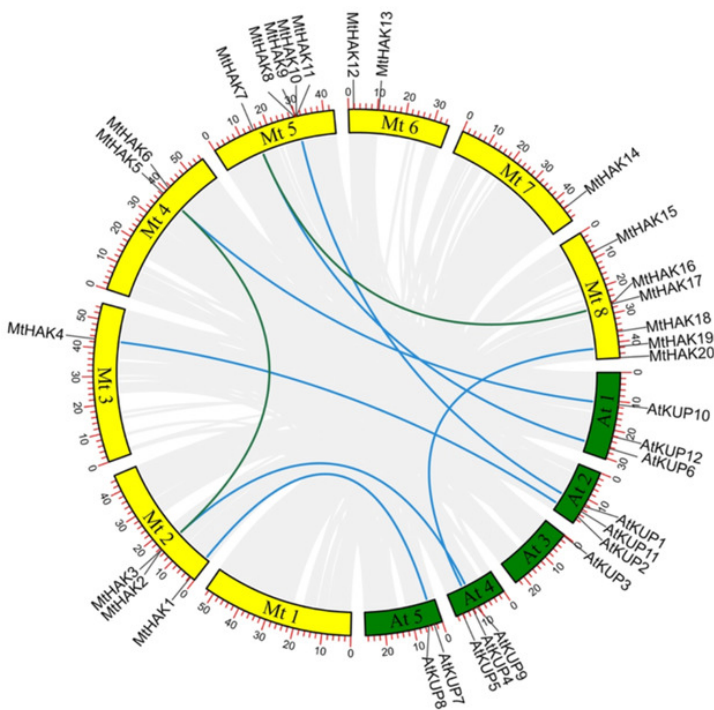
Figure 4

Analysis of the *cis*-acting regulatory elements in the promoter region of the *MtHAK* genes.

Depending on the functional annotation, the elements were classified into three main categories: phytohormone-responsive, abiotic stress-responsive, and plant growth and development-related. The frequency of these elements in the promoter region was represented by the numbers and the depth of the red color.

	Phytohormone responsive									Abiotic stress									Growth and development							
	TCA-element	AuxRR-core	GARE-motif	P-box	ERE	ABRE	TGACG-motif	TGA-element	CGTCA	STRE	ARE	WRE3	MBS	WUN-motif	LTR	DRE-core	TC-rich repeats	DRE1	O2-site	GCN4	CAT-box	AACA_motif	RY-element	CCGTCC-box	MSA-like	HD-Zip 1
MtHAK1				2	2	8		1		1	4			4					1	1						
MtHAK2	1				1		1		1	1			1	1												
MtHAK3				1		4	1	1	1	1	1		1						1	1	1	1	1			
MtHAK4						4				1	3										1	1		2		
MtHAK5		1		1				1			3		1	2			2			1						
MtHAK6	1			1	1	3	3		3	3	2			1	1	1			1							1
MtHAK7	3						1	1	1			1	2	1					1							
MtHAK8	2				1	2	2		2			1	1													
MtHAK9	1				1	1	1	1	1	1		1					2	1								
MtHAK10	1										1			1												
MtHAK11	2				2	1	1		1	2	1		1	1												
MtHAK12				1			1		1	1	3				1		1		1							
MtHAK13					3		1	1	1	1	2	1	2	1					1						1	
MtHAK14	1				1	2	2		2		2		1					1								
MtHAK15	2					1		1		1	1	2	1	1								1				
MtHAK16					4	4	2	1	2	2	2							1	1							
MtHAK17	1	1	1		1		3	1	3	1	3	1	2	1					2					4		
MtHAK18					2	3					1	2			1		1									
MtHAK19	2				3	2	3		3	5			1	1			1					3		2		
MtHAK20																										

Figure 5

Expression patterns of the *MtHAK* genes in different developmental tissues.

The microarray data were normalized based on the mean value of each gene in all the analyzed plant organs. The heat map was portrayed by the relative expressions after $\log_2$ transformed.
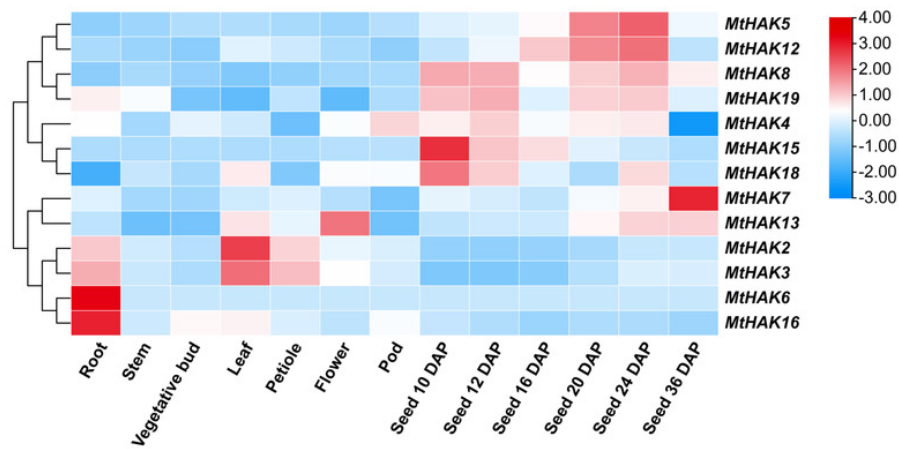
Figure 6

Relative expression of the *MtHAK* genes in response to K$^+$ deficiency treatment.

Two-week-old seedlings were placed in K$^+$ deficient conditions for 0, 1, 6, 12, 24, and 48 h. Mean values and standard errors were calculated from three biological replicates. * indicates the significant difference between K$^+$ deficiency and control at $p < 0.05$.
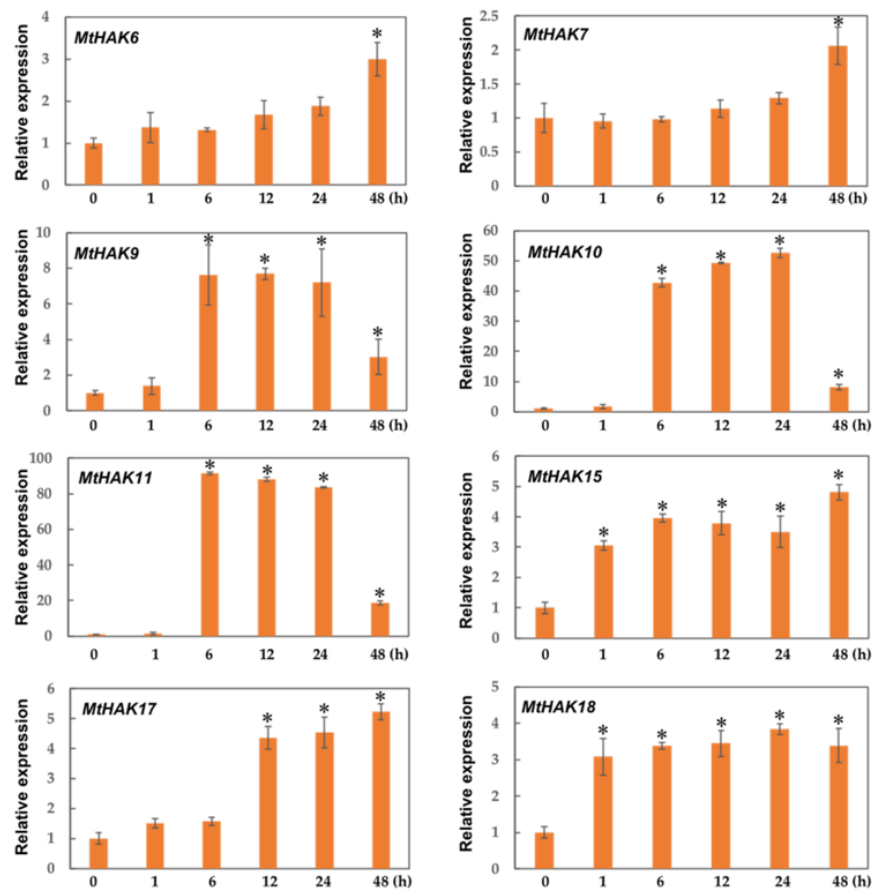
Figure 7

Relative expression of the *MtHAK* genes in response to salt stress.

Two-week-old seedlings were treated with 300 mM NaCl for 0, 1, 6, 12, 24, and 48 h. Mean values and standard errors were calculated from three biological replicates. *indicates the significant difference between the salt-stressed and control at $p < 0.05$.
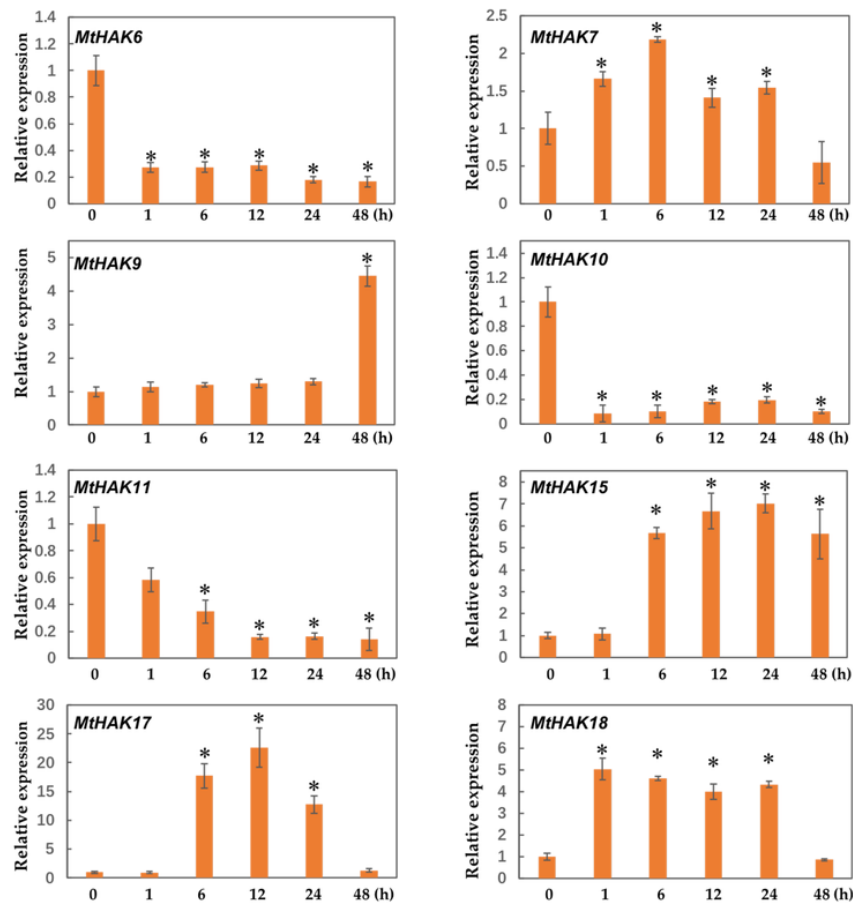
Figure 8

Relative expression of the *MtHAK* genes in response to drought stress.

Two-week-old seedlings were treated with 18% PEG6000 for 0, 1, 6, 12, 24, and 48 h. Meanvalues and standard errors were calculated from three biological replicates. *indicates the significant difference between the drought-stressed and control at $p < 0.05$.